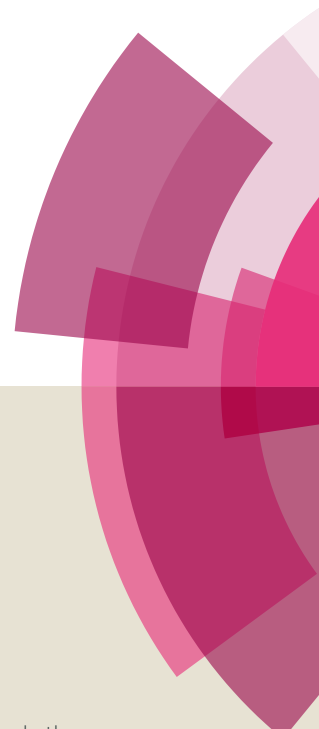


NJC

Accepted Manuscript



This article can be cited before page numbers have been issued, to do this please use: A. P. Shah, A. Sharma, S. Jain and N. G. Shimpi, *New J. Chem.*, 2018, DOI: 10.1039/C8NJ00410B.



This is an Accepted Manuscript, which has been through the Royal Society of Chemistry peer review process and has been accepted for publication.

Accepted Manuscripts are published online shortly after acceptance, before technical editing, formatting and proof reading. Using this free service, authors can make their results available to the community, in citable form, before we publish the edited article. We will replace this Accepted Manuscript with the edited and formatted Advance Article as soon as it is available.

You can find more information about Accepted Manuscripts in the [author guidelines](#).

Please note that technical editing may introduce minor changes to the text and/or graphics, which may alter content. The journal's standard [Terms & Conditions](#) and the ethical guidelines, outlined in our [author and reviewer resource centre](#), still apply. In no event shall the Royal Society of Chemistry be held responsible for any errors or omissions in this Accepted Manuscript or any consequences arising from the use of any information it contains.

Microwave assisted one pot three component synthesis of propargylamine, tetra substituted propargylamine and pyrrolo[1,2-a]quinolines using CuNPs@ZnO-PTh as a heterogeneous catalyst

Akshara P. Shah^a, Anuj S. Sharma^b, Shilpa Jain^a and Navinchandra G Shimpi^{a,*}

^aDepartment of Chemistry University of Mumbai, Santacruz (East), Mumbai-400098, India

^bDepartment of Chemistry, School of Sciences, Gujarat University, Ahmedabad-380009, India

Abstract

The present work deals with the investigation and catalytic activity of copper nanoparticles (CuNPs) supported on Zinc oxide-polythiophene (ZnO-PTh) nanocomposite. CuNPs@ZnO-PTh was prepared using simple impregnation method and characterized using various techniques (XRD, XPS, FT-IR, SEM, ICP-AES, TEM, TEM-EDS and EDAX). HR-TEM indicates that CuNPs supported on ZnO-PTh were of spherical in shape and distributed uniformly over the nanocomposite with particle size ~2-8 nm. Further, synthesized CuNPs@ZnO-PTh was used as a heterogeneous catalyst for the synthesis of propargylamine, tetra substituted propargylamine (A³ and KA² coupling reactions) and pyrrolo[1,2-a]quinoline (A³ coupling reactions) using microwave technique in ethylene glycol as a recyclable, green and biodegradable solvent with 98% yield. The high catalytic activity of CuNPs@ZnO-PTh was due to the high surface area and synergetic effect of both CuNPs and ZnO-PTh nanocomposite, which makes it cost effective, environmentally benign with high atom economy. Considering all above facts, this protocol was found to be more efficient and sustainable as compared to available commercial methods.

Keywords: CuNPs@ZnO-PTh, KA² and A³ coupling, Heterogeneous catalyst and Reusability

*Corresponding author:

Dr. Navinchandra G. Shimpi(navin_shimpi@rediffmail.com)

Phone No: +91-22-265435

Introduction

With increasing environmental concerns and economic considerations, there is a huge demand for inexpensive and abundant base metals among novel catalytic materials in replacement of expensive precious metals.¹ Among base-metal nanoparticles, copper nanoparticles (CuNPs) display unique catalytic reactivity in a wide range of organic transformations such as hydrogenation², cross-coupling reactions³, reduction⁴, azide-alkyne cycloaddition⁵ and oxidation reactions.⁶⁻⁷ Copper metal can exist in various possible oxidation states such as Cu⁰, Cu⁺¹ and Cu⁺² etc. which enables one and two electron transfer mechanism.⁸ The CuNPs display several advantages such as highly accessible surface areas and unique quantum effects which are significant for any catalytic reactions. Generally, CuNPs with smaller sizes are preferred since particle size of less than 10 nm with a narrow size distribution is believed to be most beneficial for catalytic efficiency. However, the increase in surface energy with decreasing particle size certainly causes serious aggregation, thereby leading to inferior performance in practical applications. The major problem is to stabilize copper nanoparticles and prevent its oxidation and agglomeration.⁹ Thus, need of the hour is to develop various support materials which can stabilize the copper nanocatalyst and also shows higher stability, selectivity and are cost-effective.¹⁰ Considering this, ZnO-PTh nanocomposite was prepared as support material using simple impregnation method. Synergistic effect in catalytic activities of ZnO-PTh with Cu are the main reasons for enhancement in catalytic activity along with high surface area.¹¹

Microwave (MW) are known as non-ionizing radiations, namely electromagnetic waves that are composed of mutually perpendicular electric and magnetic fields. MW heating is non-contact energy transfer process that alters electromagnetic energy into thermal energy at certain frequencies, comprising fast heating rates. In addition, electromagnetic energy is effectively absorbed by the materials under microwave irradiation. In heterogeneous catalyzed organic reactions, the uses of MW is increasing significantly and playing a crucial role which provides environmentally benign approach in terms of sustainable chemistry among scientific community. The main advantages associated with MW are remarkably reduced reaction time, reduced formation of by products and improved yield with purity of the desired product.¹²⁻¹³

Presently, the multicomponent coupling reactions became a powerful synthetic tool for the synthesis of valuable organic compounds by using supported heterogeneous catalyst.¹⁴⁻¹⁵

However, it was challenging to develop such sustainable and green tool for the synthesis of multicomponent reaction which follows the green metrics factor such as the higher atom economy with low-E factor. Environmental factor (E-factor) is the most important principle in green chemistry that calculates the total waste amount produced after purification of desired product. Therefore, researchers have put efforts to design such catalyst, which shows higher activity, selectivity in green and reusable solvents with excellent reusability up to several cycles without loss in activity.

Amongst the available multicomponent reactions, significant efforts have been made for the one pot A^3 and KA^2 coupling reaction of secondary amine, aldehyde or cyclic ketone and alkyne to synthesize propargylamines and tetra-substituted propargylamine.¹⁶ Propargylamines were synthesized traditionally by the amination of propargylic halides, propargylic phosphonates, propargylic triflates and the nucleophilic addition of in situ generated metal acetylides to imines and enamines.¹⁷⁻¹⁹ This method had several disadvantages such as poor atom economy, corrosive, generation of large amounts of waste after the completion of reaction, use of stoichiometric amounts of reagents which are highly sensitive towards the moisture and it requires tedious workup procedure during the reaction. Propargylamines has wide applications and plays a crucial role in various biologically active compounds such as oxazoles, isosters, oxotremorine analogues and conformational restricted peptides. In addition, it is also used as intermediate for the production of natural products such as β -lactams, herbicides and fungicides. Propargylamines are useful in synthesis of various drug molecules for treatment of Parkinson's and Alzheimer's disease. Moreover, it shows remarkable biological activity and has been successfully applied in drugs such as rasagiline which is a potent cardiovascular drug.²⁰⁻²² Additionally, among the various propargylamines, amines functional groups present on propargylamine intermediates were found to be most versatile precursors to develop biologically important heterocycles such as quinolines, aminoindolizines, pyrrolo[1,2-a]quinolines etc.²³ It was found that the pyrrolo[1,2-a]quinolines is a tricyclic heterocyclic compound mainly found in natural products with a wide range of biological activities such as antibacterial, antifungal, apoptosis, anticonvulsant, anti-inflammatory, anti-leukemic, histamine H3 receptor antagonist activity, neurological activities and tumour inhibitor against P388 leukaemia (Figure 1).²⁴

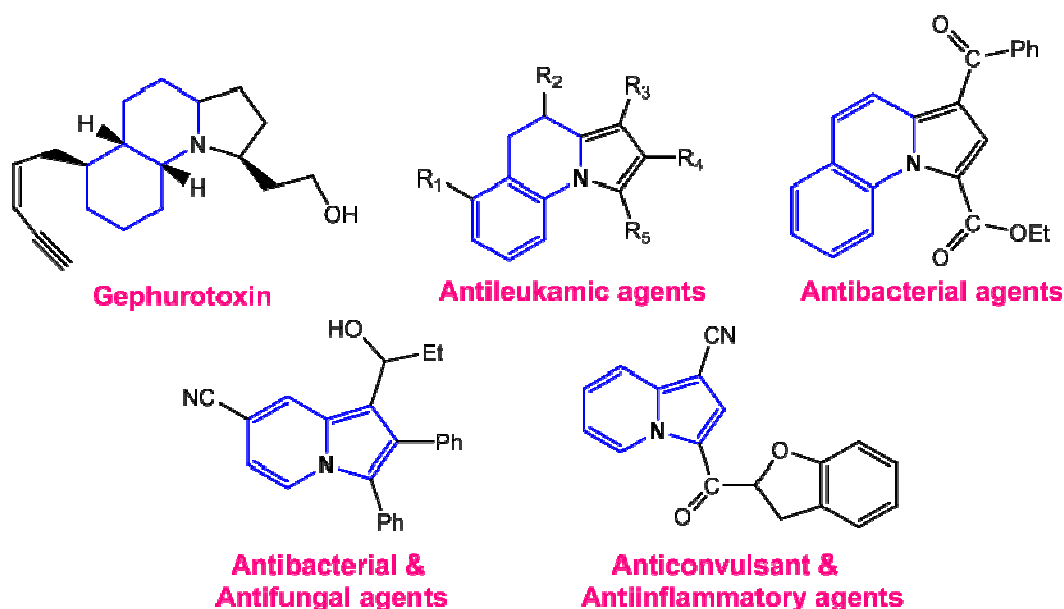


Figure 1 Biologically important pyrrolo[1, 2-a]quinoline containing natural product and pharmaceuticals

The yield of propargylamine has been improved using various homogenous catalysts such as Cu(I) pybox complex²⁵, dicopper (I) complex²⁶, Fe-I₂-CuBr²⁷, Cu-PF₆ ligand²⁸, CuCl₂²⁹, CuBr³⁰, CuI³¹ and CuCl.³²⁻³³ However poor reusability, lower stability and water contamination reduces its applicability in various industries as well as academics. To overcome this limitation, various heterogeneous catalysts such as Cu-CMC³⁴, SiO₂-NHC-Cu(I)³⁵, CuNPs@ MS³⁶, CuNPs/TiO₂³⁷, Cu(II)/HM³⁸, CuO/Fe₂O₃³⁹⁻⁴⁰, Cu(I)-N₂S₂-salen/MCM-41⁴¹, Cu(I)-USY (zeolite)⁴², CuO/GNS(graphene)⁴³⁻⁴⁴, CuNPs@Fe₃O₄NPs/GO⁴⁵, CuNPs/Montmorillonite⁴⁶, CuI/TrititanateNanotube⁴⁷, Cu₂O/ZnO⁴⁸ and Cu/Al-oxide⁴⁹ etc. are used for A³ as well as KA² coupling reactions. Xiong et al. developed oyster shell waste supported CuCl₂ catalyst and investigated its activity towards A³ coupling under the microwave irradiations.⁵⁰ Nevertheless, the issues of recyclability reduced its applicability. Recently, Ermolatev et al. reported microwave assisted decarboxylative coupling of 2-oxaacetic acid, an amine and alkyne to form poly-substituted propargylamine using CuBr as catalyst. However, both methods required high amount of catalyst loading (15 mol%) and recyclability issues, which makes this protocol less sustainable and accessible.⁵¹ Tu et al. reported an efficient tool to synthesize propargylamine under microwave irradiation using CuI catalyst.⁵² Similarly, Kaur et al. reported microwave assisted synthesis of propargylamine by employing CuNPs supported on nitro-functionalized

polystyrene resin (NPS). This catalyst gave higher yield of propargylamine in shorter reaction time. However, the utilization of toluene as solvent and higher copper loading was required for higher yield of product.⁵³

Herein, we report, synthesis and catalysis of CuNPs@ZnO-PTh nanocomposite for A^3 and KA^2 coupling reactions for the synthesis of propargylamines, tetra substituted propargylamine and pyrrolo[1,2-a]quinolines using microwave technique. This synthetic protocol may offer potential route using catalytic amount as well as acts as a versatile, heterogeneous and recyclable catalyst, which shows higher yield and high atom economy.

Experimental

Materials and method

All chemicals and reagents were purchased from commercial sources and used without further purification. Reactions were performed in a microwave at 100°C. Column chromatography was carried out using silica gel (230-400 mesh). Thin layer chromatography was performed using Merck silica gel 60 F254 plates (TLC) and components were visualized using UV (254 nm). Melting points were taken in open capillaries and are uncorrected. The crystalline or amorphous nature of ZnO, ZnO-PTh and CuNPs@ZnO-PTh was analysed using powder X-ray diffractometer (Shimadzu, Maxima 7000 S) using $CuK\alpha$ ($\lambda=1.5418 \text{ \AA}$ and 1.6 kW X-ray tube with applied voltage of 40 kV and current values of 40 mA) radiation from 10 to 80° 2 θ range at scanning speed of 5° min⁻¹. Diffraction peaks of crystalline phases were compared with standard JCPDS data files. XPS data was obtained using monochromatic aluminium with an Al $K\alpha$ (1486.6 eV) with X-ray source operating at a vacuum of 10⁻⁷ Pa. All the binding energy values were calibrated using C1 s line of 284.7 eV. Isolated products were confirmed using Fourier transform infrared (FTIR) spectroscopy recorded on Perkin Elmer, Frontier equipment. Morphology and particle size of the samples were investigated on field emission scanning electron microscope (FESEM, Hitachi S-4800, Japan). Inductively coupled plasma atomic emission spectroscopy (ICP-AES) analysis was carried out on a HJY Ultima-2 instrument: 1000 W, nebulizer pressure 2.96, nebulizer flow 1.29, wavelength 242.795 nm. A JEOL JEM 2100 instrument was used for particle size measurements through transmission electron microscopy (TEM) as well as energy dispersive atomic X-ray analysis (EDAX). ¹H and ¹³CNMR (300Hz)

was recorded on Bruker ADVANCE II using TMS as internal standard in CDCl_3 . ESI Mass spectra of representative compounds were recorded on a Waters UPLC-TQD Mass spectrometer.

Synthesis of ZnO nanorods

Zinc chloride (ZnCl_2) (1.0 M), NaOH (4.0 M) and sodium dodecyl sulphate (SDS) (0.2 M) solutions were prepared in deionized water respectively. According to the molar ratio of $\text{Zn}^{2+}/\text{OH}^-$, NaOH (4M) was added drop-wise into 1M ZnCl_2 (20mL) aqueous solution with intense magnetic stirring at 3°C . Further, 5mL SDS (0.2 M) and 40mL distilled water were introduced into the above mixture to get a 100mL clear solution. Thereafter, the solution was kept at room temperature for 1.5 hours under vigorous stirring to obtain white precipitate. Subsequently, the solution was transferred to ground-glass stopped conical flask and aged at 85°C for 5h. The precipitate deposited on the bottom of the conical flask were collected by centrifugation and repeatedly washed with water and ethanol. Precipitates obtained were dried at 60°C in vacuum oven⁵⁴.

Synthesis of ZnO- PTh nanocomposite

ZnO NRs (1 gm) were dispersed in chloroform (20 ml) and sonicated for 30 min. Further 1.6 ml (0.02 mol) of thiophene was added in ZnO NRs solution and stirred for 30 min with drop-wise addition of FeCl_3 solution prepared in chloroform. The ratio of FeCl_3 to thiophene was taken as 3:1. Further the solution kept for next 24 h at room temperature under controlled stirring. The obtained composite was filtered and washed multiple times with water to remove unreacted oxidising agent. Further, composite was washed with methanol to convert it into reduced state (black to red). The obtained precipitate was dried in hot air vacuum oven at 50°C for 4 h.⁵⁵

Synthesis of CuNPs@ZnO-PTh

ZnO-PTh nanocomposite (1.0 g) was dissolved in deionised water (20 ml) with constant stirring. $\text{CuNO}_3 \cdot 3\text{H}_2\text{O}$ (1.0 mmol) solution prepared in deionised water was added drop-wise to the solution of ZnO-PTh. While stirring, hydrazine hydrate (2.0 mmol) was added slowly and solution was kept under constant magnetic stirring for 4 h. The resulting colloidal suspension was centrifuged and washed multiple times using deionised water. Further, the as obtained catalyst was dispersed in water (10 ml) and stored under inert condition.

General reaction procedure for A^3 and KA^2 coupling catalyzed by Cu NPs@ ZnO-PTh

A mixture of aldehydes (1.0 mmol) or cyclic ketones (1.0 mmol), secondary amines (1.0 mmol), acetylenes (1.0 mmol), CuNPs@ ZnO-PTh (20 mg) and ethylene glycol (2ml) were added to a 10ml CEM vial and stirred at 80°C for 15 minutes. After completion of reaction (monitored by TLC) reaction mixture was centrifuged and filtered. Then, the reaction mass was dissolved in ethyl acetate. The ethyl acetate layer was washed with water (3 x 10ml) and brine (1 x10 ml) and treated with dried anhydrous Na_2SO_4 . The reaction mixture was concentrated under vacuum and crude reaction mass was purified by column chromatography using hexane-ethyl acetate as the eluent.

Results and discussion

Characteristics of ZnO-PTh

ZnO-PTh nanocomposite was selected as support for deposition of CuNPs. Polymeric materials have been effectively used as a promising support for the stabilization of metal nanoparticles with control over size distribution. The purpose of using support of ZnO-PTh is to make the CuNPs free from aggregation, as aggregation leads to decrease in surface to volume ratio, which ultimately decreases its catalytic properties.⁵⁶ Polythiophene is an organic conducting polymer with good chemical stability, mechanical strength and bio-compatibility. While, ZnO is a well-known n-type semiconductor with band gap of 3.37 eV. This inorganic-organic hybrid structure exhibits excellent physicochemical properties resulting from synergistic effect of individual properties of semiconducting metal oxide (ZnO) and conducting polymer (PTh). Interactions occurring at molecular levels and nano-meter size control of these hybrid materials leads to an efficient electron-transfer reaction which is crucial for any catalytic process. The well-dispersed ZnO-PTh nanocomposites were produced in a single reaction step. This method has several advantages over existing techniques as it does not require templates and large amount of organic solvents. Synthesized composites were used as a support for Cu nanoparticle as shown in Figure 2.

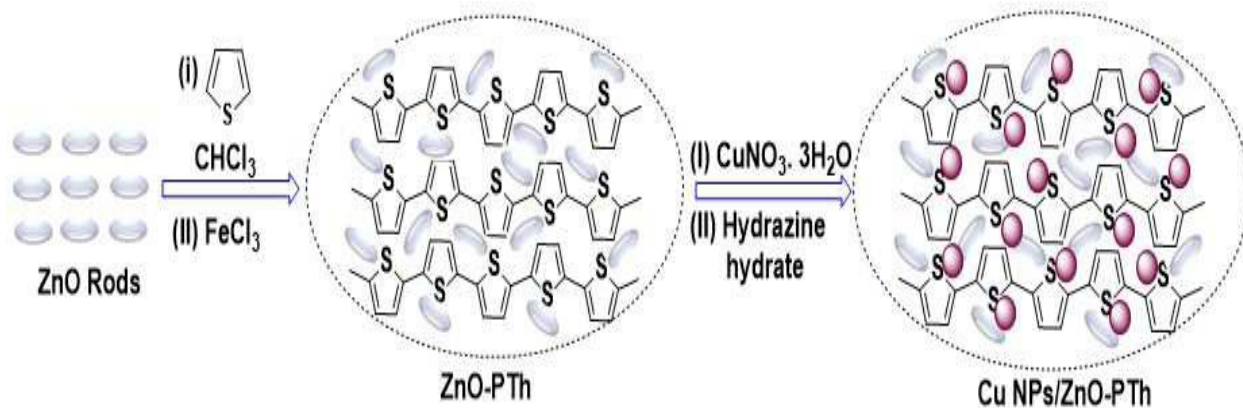


Figure 2 Schematic representation for the synthesis of CuNPs@ZnO-PTh

Characterization of CuNPs@ZnO-PTh

The synthesized CuNPs@ZnO-PTh catalyst was thoroughly characterized by various sophisticated analytical techniques such as, XRD, XPS, FT-IR, FESEM, TEM, EDS and EDAX. XRD of ZnO NRs shows similar diffraction peaks, which corresponds to hexagonal wurtzite phase (JPCDS 36-1451, Figure 3a).⁵⁷ Average particle size was calculated using Scherrer's formula and found to be ~25 nm. However, diffraction peak of ZnO was absent in ZnO-PTh nanocomposite and only broad diffraction peak was observed at $2\theta = 15-25^\circ$ (Figure 3b). The ZnO peak gets disappeared completely in ZnO-PTh nanocomposite since ZnO gets embedded into PTh chains, thus affecting the detection of crystal diffraction.⁵⁴ Figure 3c shows the diffraction pattern of CuNPs@ZnO-PTh, peaks observed at 43.52° , 50.64° and 74.35° corresponds to (111), (200), and (220) planes of fcc structure of pure Cu (JCPDS no. 71-4610), while peaks of lesser intensity before 43.52° matches with ZnO-PTh (Figure 3c).⁵⁸⁻⁵⁹ This suggests that CuNPs were decorated over the surface of ZnO-PTh support.

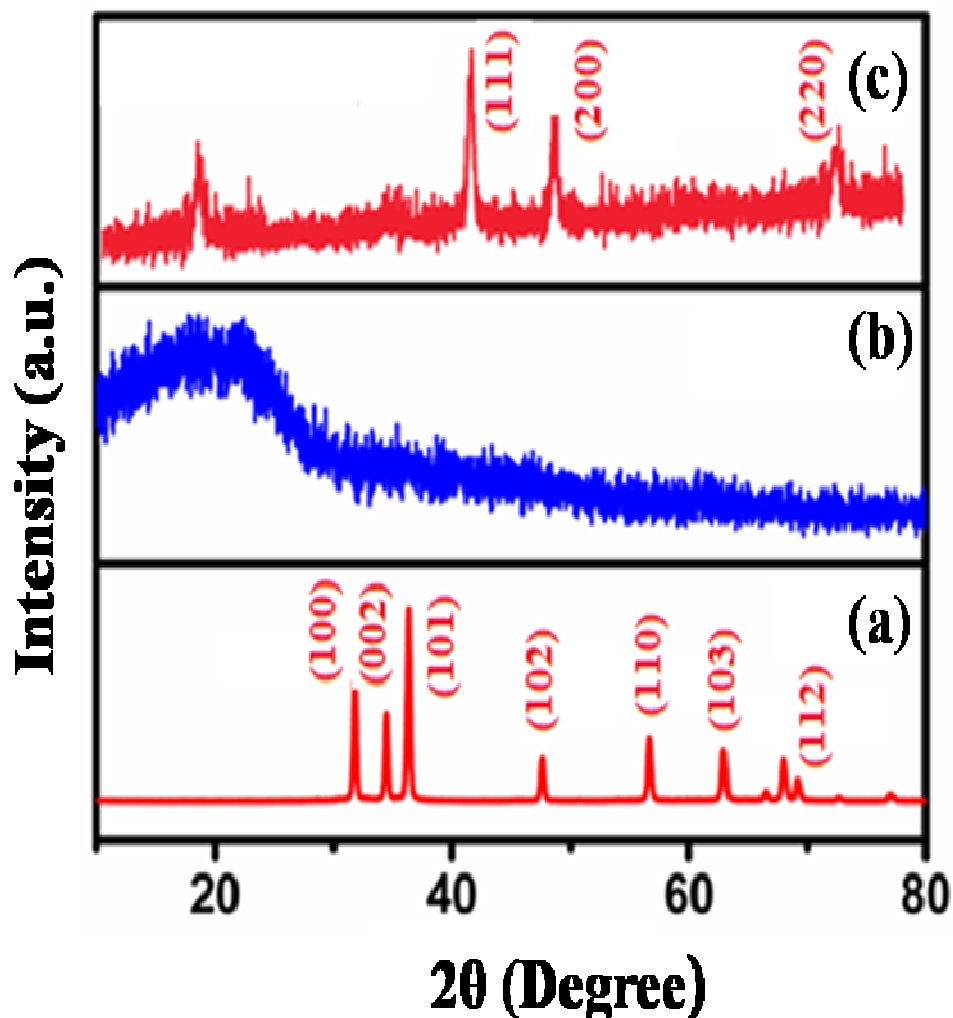


Figure 3 XRD of (a)ZnO, (b)ZnO-PTh and (c) CuNPs@ZnO-PTh

The oxidation state and surface property of copper nanoparticles supported on ZnO-PTh nanocomposite and its elemental composition was investigated by X-ray photoelectron spectroscopy. The survey spectra revealed the presence of Cu 3p, O 1s, C 1s, Zn 2p and S 2p with binding energies at 932.05 eV, 530.6 eV, 286 eV and 163.2 eV respectively. (Figure S1, See ESI). The deconvoluted C1s binding energy spectrum was fitted into three peaks at around 284.6 eV, 286.2 eV and 288 eV, which can be attributed to C-C, C-S, C=C bonding, respectively (Figure S2, See ESI). The XPS spectrum for Zn 2p core-level consisting of Zn 2p_{3/2} and 2p_{1/2} peaks at 1021.28 eV and 1044.45 eV, attributed to Zn²⁺ valance state (Figure S3, See ESI).⁶⁰ The O1s peak appeared at 530.10 eV was due to the presence of Cu-O bond (Figure S4, See ESI). In addition, peak observed at 531.53 eV was due to oxide ions that are surrounded by Zn atoms.

The Zn 2p XPS spectrum was broad and asymmetric. The deconvoluted S 2p peak indicates the presence of $2p_{3/2}$ (164.1 eV) and $2p_{1/2}$ (165.3 eV) with a separation of 1.2 eV and the relatively high energy broad tail produced by positively charged sulphur within the thiophene ring (Figure S5, ESI). Further studies on XPS confirmed the presence of both Cu^{2+} and Cu reduced species as clearly visualized in Cu 2p XPS experiment (Figure 4). The presence of a shake-up peak (about 940-945 eV) was characteristic of Cu^{2+} species, particularly of CuO (in the absence of Cu^{2+}) species, no shake-up peaks can be visualized⁶¹, which is in good agreement with XRD results. The presence of lower Cu $2p_{3/2}$ binding energy peaks (932.05 eV) indicates the existence of reduced copper species.⁶² However, the distinction between Cu^+ and Cu^0 species (that appear at very similar binding energies) was only feasible through examination of the Auger spectra.⁶³

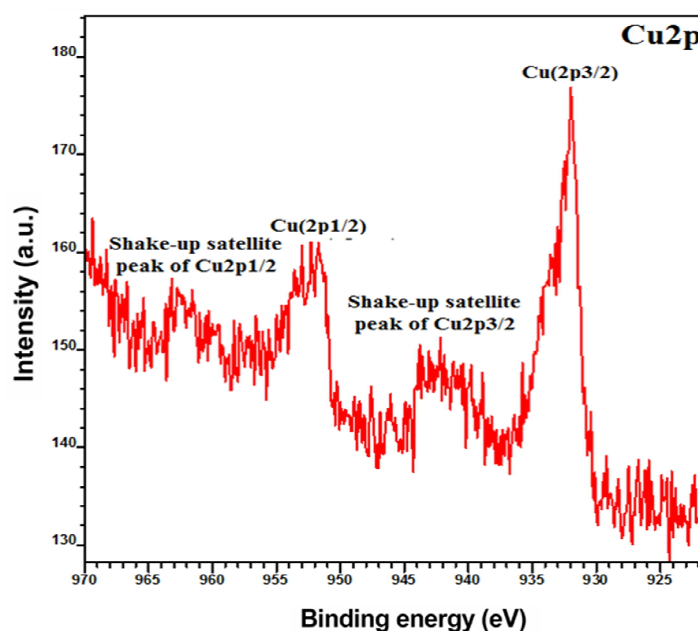


Figure 4 Deconvoluted XPS spectrum of Cu 2p

Figure 5 represents FT-IR spectra of a) ZnO, b) ZnO-PTh and c) CuNPs@ZnO-PTh respectively. The peaks observed at $3200\text{-}3600\text{ cm}^{-1}$ corresponds to O-H mode of vibration. Between 1566 and 1547 cm^{-1} , strong asymmetric stretching mode of vibration of C=O was observed (Figure 5a). In ZnO-PTh nanocomposite, a broad band appears $\sim 3423\text{ cm}^{-1}$ which corresponds to the O-H stretching vibration. The bands observed at 2923 cm^{-1} corresponds to C-H stretching vibration while bands at 1640 cm^{-1} and 1426 cm^{-1} indicate asymmetric and symmetric stretching vibrations

of thiophene units, respectively. The band at 1167 cm^{-1} and 790 cm^{-1} can be assigned to C-H (in-plane) and C-H (out-of-plane) bending vibration of thiophene units, which indicates the α -position linkage between the thiophene rings. Moreover, the bands observed at 830 cm^{-1} and 692 cm^{-1} may be assigned to C-S stretching and C-S-C bending vibrations indicating the presence of thiophene rings.⁵⁵ Figure 5b indicates the presence of ZnO in hybrid material indicated by a new band centred at 488 cm^{-1} which associates with Zn-O stretching. Similar peaks were observed in CuNPs@ZnO-PTh nanocomposite.

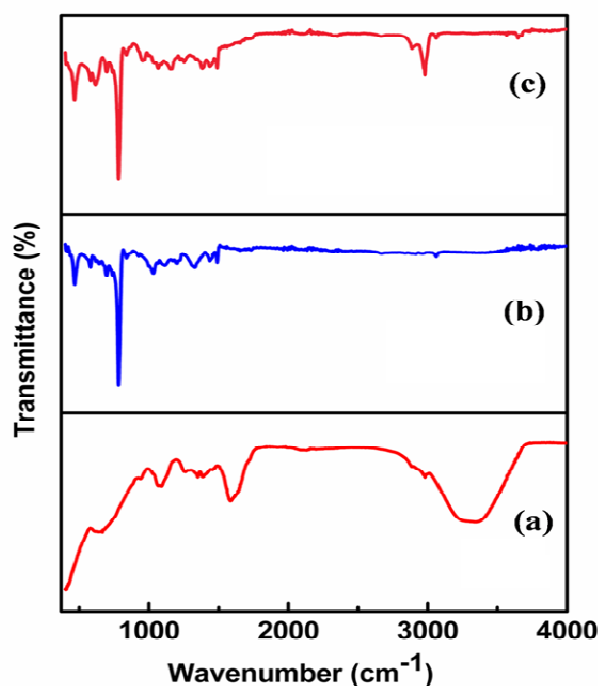


Figure 5 FT-IR of (a) ZnO, (b) ZnO-PTh and (c) CuNPs@ZnO-PTh

To evaluate the specific surface area, the nitrogen sorption measurement was carried out. Specific surface area was found to be 19.26, 35 and $71.03\text{ m}^2\text{g}^{-1}$ respectively for ZnO, ZnO-PTh and CuNPs@ZnO-PTh nanocomposite. In BET equation, when $P/P_0 \ll 1$ and $c \gg 1$, it leads to monolayer formation and Type I adsorption isotherm was obtained. The sorption exhibits type I isotherm, which indicated monolayer adsorption in our case. High surface area of CuNPs@ZnO-PTh nanocomposite leads to more active sites per unit volume, which increases catalytic efficiency. Thermal stability study was done using TGA (Figure S6, See ESI). As indicated by thermogram, thermal stability of nanocomposite increased with incorporation of CuNPs into

ZnO-PTh matrix. Catalyst doesn't show any air or moisture sensitive nature, therefore no extra care was taken in order to store or handle the catalyst in recovery process.⁶⁴⁻⁶⁵

Figure 6 shows FESEM images of a) ZnO-PTh and b) CuNPs@ZnO-PTh with sheet like structure with size in range ~200 nm (ZnO-PTh) and ~50 nm (CuNPs@ZnO-PTh) respectively. It was observed that size of nanocomposite decreases significantly with impregnation of CuNPs, which leads to increase number of active sites per unit area. Therefore, it's catalytic activity increases effectively. FESEM indicates that CuNPs have been distributed uniformly over the ZnO-PTh support, which can also be reflected from XRD pattern (Figure 3c). The amount of CuNPs loaded into the ZnO-PTh material was investigated using ICP-AES analysis. In this process, CuNPs@ZnO-PTh(500 mg) was incinerated in a crucible at 550 °C for 2h. Further, the obtained residue was dissolved in aqua regia (1 ml) and diluted using distilled water (5 ml). The average concentration of copper (3 trials) as determined from ICP-AES was found to be 0.13 mol% of copper.

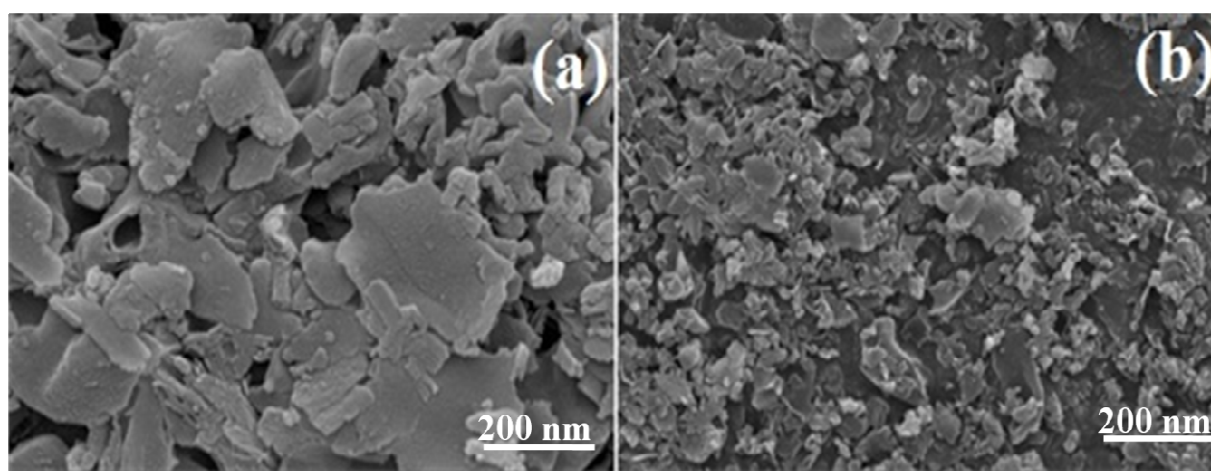


Figure 6 SEM images of (a) ZnO-PTh and (b) CuNPs@ZnO-PTh

Figure 7 represents TEM and HR-TEM of CuNPs@ZnO-PTh catalyst, respectively. It was observed that CuNPs were spherical in shape and dispersed uniformly into ZnO-PTh support. The size was observed to be ~2-8 nm. HR-TEM also supports the results of TEM i.e. CuNPs dispersed uniformly over the ZnO-PTh support. Moreover, lattice fringes with the crystal lattice

spacing of CuNPs having size 0.207 nm. The presence of Cu with uniform distribution of CuNPs into ZnO-PTh was observed on EDS mapping as well as EDAX spectra (Figure 8 and 9).

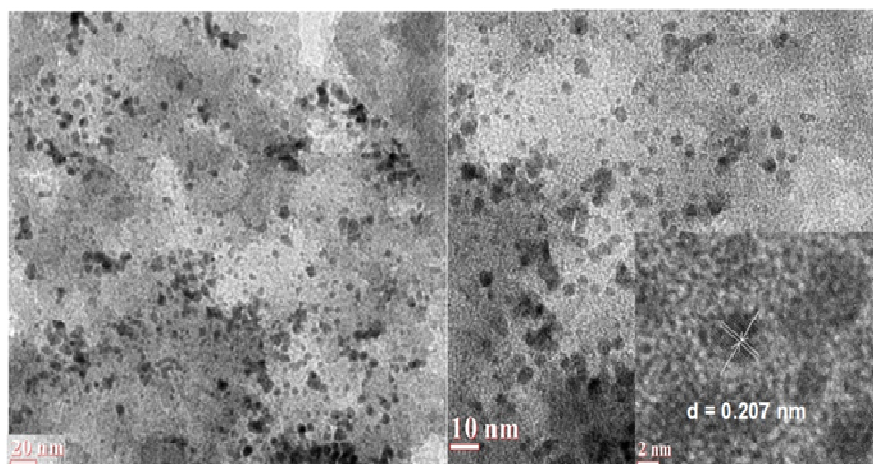


Figure 7 TEM and HR-TEM images of CuNPs@ZnO-PTh

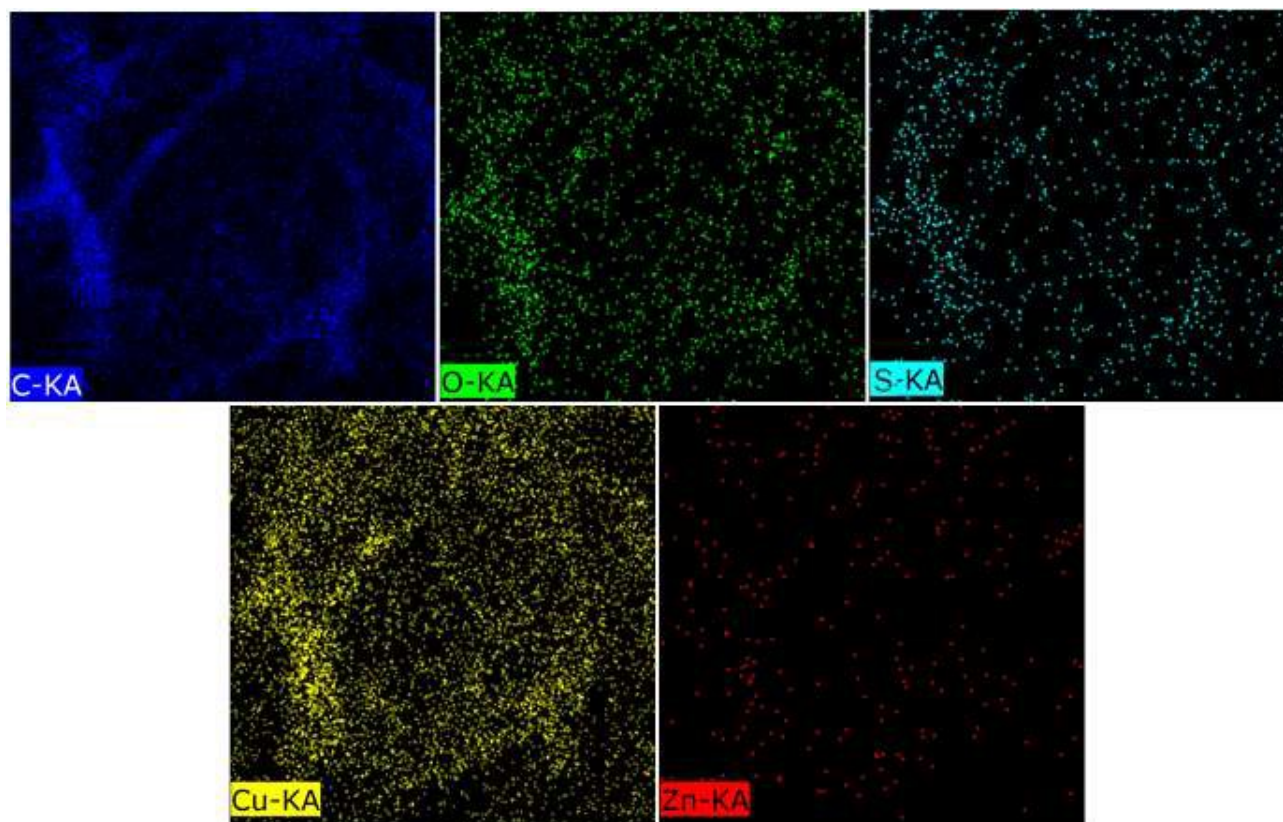


Figure 8 TEM-EDS mapping of C, O, S, Cu and Zn present in CuNPs@ZnO-PTh material

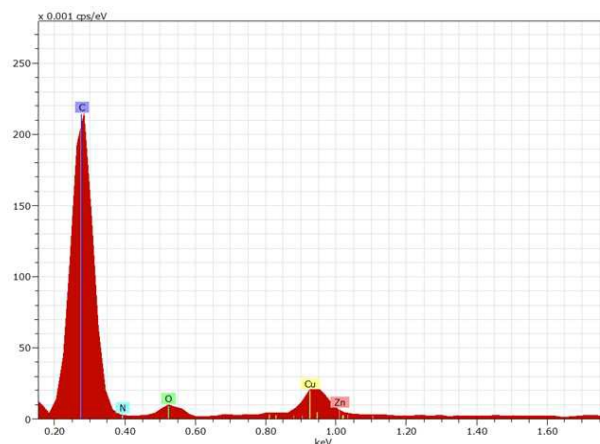
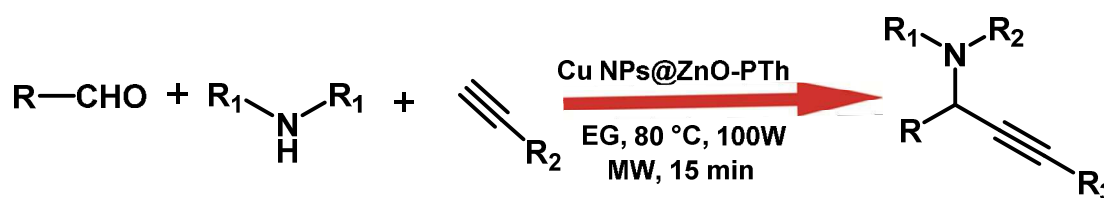


Figure 9 EDX spectra of CuNPs@ZnO-PTh

Catalytic performance of CuNPs@ZnO-PTh as a heterogeneous catalyst for one pot three component A³ coupling reactions

The initial evaluation of the catalytic activity was started with the coupling reaction of aldehydes, secondary amines and terminal acetylenes under microwave irradiation to afford propargylamines as shown in Scheme 1. The performance of supported metal nanocatalyst in organic reactions mainly depends upon the accessibility of the available catalytic sites, which mostly depends on the nature of support material, polarity of substrate as well as solvents. To study the optimized reaction conditions, a model reaction of benzaldehyde, piperidine and phenyl acetylene was performed under microwave using CuNPs@ZnO-PTh catalyst in the presence of various solvents at 80°C to afford the corresponding propargylamine as shown in Table 1.



Scheme 1 Cu NPs@ZnO-PTh Catalyzed Synthesis of Propargylamines via A³ Coupling Reaction.

The obtained product shows lower yield in polar solvents such as ethanol, acetone (47-54%) (Entries 1-2, Table 1). However, yield increased up to 64-87% in case of DMF, acetonitrile, Toluene and 1,4-dioxane solvents (Entries 3-6, Table 1). Further the reaction was carried out in

solvent free conditions, which showed poor conversion (25%). This can be attributed to the fact that most of catalyst material was stuck on the surface of microwave vials (Entry 8, Table 1). Interestingly, the desired product was obtained with 98% yield in ethylene glycol (EG) (Entry 7, Table 1). With these interesting observations, we studied the effect of temperature (entry 9-12, Table 1) and CuNPs@ZnO-PTh catalyst dose (Entry 14-16, Table 1) on the yield of product. In absence of catalyst, trace conversion was observed (Entry 13, Table 1). The present model reaction was carried out with copper nanoparticles alone as a catalyst. However, the lower yield of product was observed. This is mainly due to the instability and agglomeration of the nanoparticles during the reaction (Entry 17, Table 1). Furthermore, the reaction was also performed in the presence of ZnO-PTh support material alone as a catalyst. However, the trace yield of product was obtained (Entry 18, Table 1). The results shows that the usage of 20mg of CuNPs@ZnO-PTh catalyst at 80°C in EG was sufficient to obtained the highest yield of desired product in minimum reaction time (98 %, 15 min) (Entry 12, Table 1).

Table 1 Optimization reaction condition for CuNPs@ZnO-PTh catalyzed A³ coupling reaction^a

Entry	Catalyst (mg)	Solvent	Time (min)	Temp(°C)	Yield (1)(%)

1	20	EtOH	15	80	54
2	20	Acetone	15	80	47
3	20	DMF	15	80	64
4	20	Acetonitrile	15	80	75
5	20	Toluene	15	80	85
6	20	1,4-dioxane	15	80	87
7	20	EG	15	80	98
8 ^b	20	-	15	80	25
9	20	EG	30	50	47
10	20	EG	30	60	62
11	20	EG	25	70	75
12	20	EG	15	80	98
13 ^c	-	EG	15	80	Trace
14	05	EG	15	80	45
15	10	EG	15	80	61
16	15	EG	15	80	85
17 ^d	20	EG	15	80	25
18 ^e	20	EG	30	80	Trace

^a Reaction conditions: Benzaldehyde (1.0 mmol), Piperidine (1.0 mmol), Phenyl acetylene (1.0 mmol), Catalyst (mol %), ^b = Solvent free conditions, ^c = Absence of catalyst, ^d = Presence of Cu NPs, ^e = Presence of ZnO-PTh.

The scope of the present protocol for the synthesis of propargylamine was also investigated. The different derivatives of propargylamine were synthesized (Table 2). It was observed that the reaction was uniform, irrespective of the nature of the substituents (electron withdrawing or electron donating) on the aromatic ring. A wide range of aldehyde substituents having functional groups -X (Br, Cl, I), -OH, -CH₃, -OCH₃, -NO₂ and -N(CH₃)₂ were found to be compatible with this procedure. Almost all screened substrates undergone A³ coupling easily and effectively to obtain the corresponding yield of products. Moreover, the furfuraldehyde (Entry 10, Table 2) and vaniline (Entry 6, Table 2) gave an excellent product in minimal reaction time. Different amines such as piperidine (Entry 1, Table 2), pyrrolidine (Entry 11, Table 2) and morpholine (Entry 12, Table 2) were gave higher yield of propargylamines. Acetylenes derivatives (electron

withdrawing and electron donating) were also tried for the synthesis of propargylamine, which gave the corresponding products yield of 95-99% (Entry 13-15, Table 2). Cyclopropane also gave good yield (Entry 16, Table 2). All the products were characterized using ^1H NMR and ^{13}C NMR spectra. Some of the products were also characterized by Mass Spectra, which are summarized in supporting information.

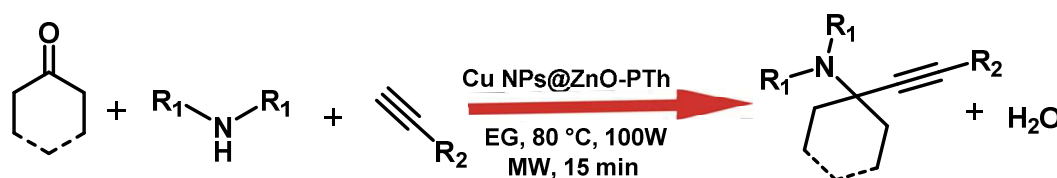
Table 2 Scope of the CuNPs@ZnO-PTh catalyst for the synthesis of Propargylamines

Entry	R (Benzaldehyde)	R ₁ (Amine)	R ₂ (Alkyne)	Yield (%)
1	Ph	Piperidine	Ph	99
2	4-Br-C ₆ H ₄	Piperidine	Ph	98
3	4-Cl-C ₆ H ₄	Piperidine	Ph	97
4	4-OH-C ₆ H ₄	Piperidine	Ph	95
5	4-NO ₂ -C ₆ H ₄	Piperidine	Ph	98
6	4-OH-3-OMe-C ₆ H ₃	Piperidine	Ph	99
7	4-I-C ₆ H ₄	Piperidine	Ph	71
8	4-OCH ₃ -C ₆ H ₄	Piperidine	Ph	74
9	4-N(CH ₃) ₂ -C ₆ H ₄	Piperidine	Ph	96
10	C ₄ H ₃ O	Piperidine	Ph	96
11	Ph	Pyrrolidine	Ph	95
12	Ph	Morpholine	Ph	92
13	Ph	Piperidine	4-Br-C ₆ H ₄	99
14	Ph	Piperidine	4-NO ₂ -C ₆ H ₄	97
15	Ph	Piperidine	4-CH ₃ O-C ₆ H ₄	95
16	Ph	Piperidine	C ₃ H ₅	78

Reaction conditions: Aldehyde (1.0 mmol), Acetylene (1.0 mmol), Secondary amine (1.0 mmol), Catalyst (20 mg), 5 mL Ethylene Glycol, 15 min, 100W.

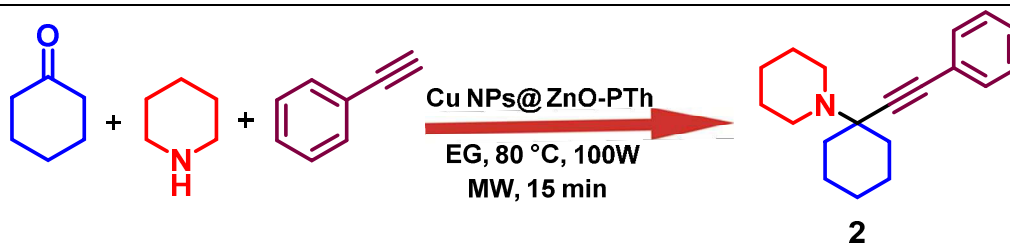
Catalytic performance of CuNPs@ZnO-PTh towards one pot three component KA² coupling reactions

Next, we investigated the catalytic activity of the CuNPs@ ZnO-PTh catalyst for the coupling reaction of cyclic ketone, secondary amines and terminal acetylenes under microwave irradiation to afford tetrasubstituted propargylamines as shown in Scheme 2. To study the optimized reaction conditions, a model reaction of cyclohexanone, piperidine and phenyl acetylene was performed under microwave using CuNPs@ZnO-PTh catalyst in the presence of various solvents at 80°C to afford the tetrasubstituted propargylamine (2) shown in Table 3.



Scheme 2 Cu NPs@ZnO-PTh Catalyzed synthesis of tetrasubstituted propargylamines via KA² Coupling Reaction

It was observed that the polar solvents such as ethanol, methanol and water gave poor yield of product (25-47%) (Entries 1-3, Table 3). The yield of product was increased up to 55-82% in DMF, acetonitrile and 1,4-dioxane (Entries 4-6, Table 3). However, the reaction was also carried out in solvent free conditions, which shows poor yield of products (Entry7, Table 3). The best yield (98%) of the desired product was achieved in ethylene glycol (EG) (Entry 8, Table 3). The effect of various parameters such as temperature (Entries 9-12, Table 3) and catalyst concentration (Entries 14-17, Table 3) were well studied. However, in the absence of the catalyst, only trace conversion was found (Entry 13, Table 3). The model reaction was also carried out with Cu NPs. However, poor yield was observed (Entry18, Table 3). In addition, the support material such as ZnO-PTh alone use as a catalyst; the trace yield of product was observed (Entry 19, Table 3). Thus, the results shows that the usage of 25mg of CuNPs@ZnO-PTh catalyst dose at 80°C in EG was sufficient to obtained highest yield of tetrasubstituted propargylamine in minimum period of time (98 %, 15 min) (Entry 8).

Table 3 Optimization reaction conditions for CuNPs@ZnO-PTh catalyzed KA² coupling reaction^a

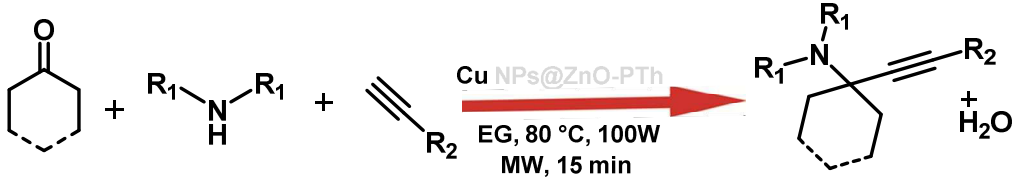
Entry	Catalyst (mg)	Solvent	Time (min)	T (°C)	Yield (2) (%)
1	25	EtOH	15	80	43
2	25	MeOH	15	80	47
3	25	H ₂ O	15	80	25
4	25	DMF	15	80	55
5	25	Acetonitrile	15	80	67
6	25	1,4-dioxane	15	80	82
7 ^b	25	-	15	80	15
8	25	EG	15	80	98
9	25	EG	35	50	45
10	25	EG	30	60	71
11	25	EG	20	70	80
12	25	EG	15	80	98
13 ^c	-	EG	15	80	Trace
14	05	EG	15	80	42
15	10	EG	15	80	62
16	15	EG	15	80	85
17	20	EG	15	80	90
18 ^d	25	EG	15	80	32
19 ^e	25	EG	30	80	Trace

^aReaction conditions: Cyclohexanone (1.0 mmol), Piperidine (1.0 mmol), Phenyl acetylene (1.0 mmol), Catalyst (mol %), ^b = Solvent free conditions, ^c = Absence of catalyst, ^d = Presence of Cu NPs, ^e = Presence of ZnO-PTh.

We expanded the scope of present catalyst CuNPs@ZnO-PTh for the synthesis of tetrasubstituted propargylamines from the reaction using various substrates such as cyclohexanone, cyclopentanone and secondary amines including piperidine, morpholine, pyrrolidine with various substituted phenyl acetylene in our optimization reaction conditions. It was also found that almost all screened secondary amine underwent KA² coupling smoothly to

afford the corresponding products in 95-98% yields. Further, the substituted phenyl acetylene gave higher yield of product (94-96%). However, the reaction proceeded slowly in case of cyclopropyl acetylene (Entry 9, 11, Table 4).

Table 4 Scope of the CuNPs@ZnO-PTh catalyst for the synthesis of tetra substituted Propargylamines



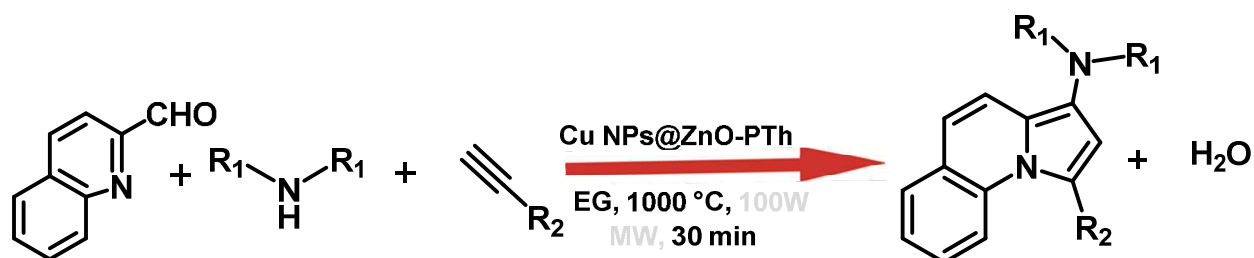
Entry	Cyclic Ketone	R ₁ (Amine)	R ₂ (Alkyne)	Yield (%)
1	Cyclohexanone	Piperidine	Ph	96
2	Cyclohexanone	Pyrrolidine	Ph	94
3	Cyclohexanone	Morpholine	Ph	95
4	Cyclopentanone	Piperidine	Ph	96
5	Cyclopentanone	Pyrrolidine	Ph	95
6	Cyclopentanone	Morpholine	Ph	94
7	Cyclopentanone	Piperidine	4-CH ₃ O-C ₆ H ₄	96
8	Cyclohexanone	Piperidine	4-CH ₃ -C ₆ H ₄	95
9	Cyclohexanone	Piperidine	C ₃ H ₅	85
10	Cyclopentanone	Piperidine	4-CH ₃ -C ₆ H ₄	97
11	Cyclopentanone	Piperidine	C ₃ H ₅	78
12	Cyclopentanone	Piperidine	4-CH ₃ O-C ₆ H ₄	95

Reaction conditions: Cyclic ketone (1.0 mmol), Secondary amine (1.0 mmol), Alkyne (1.0 mmol), Catalyst (25 mg), 5 mL Ethylene Glycol, 15 min, 100W.

Catalytic performance of CuNPs@ZnO-PTh towards the synthesis of pyrrolo[1, 2-a]quinoline

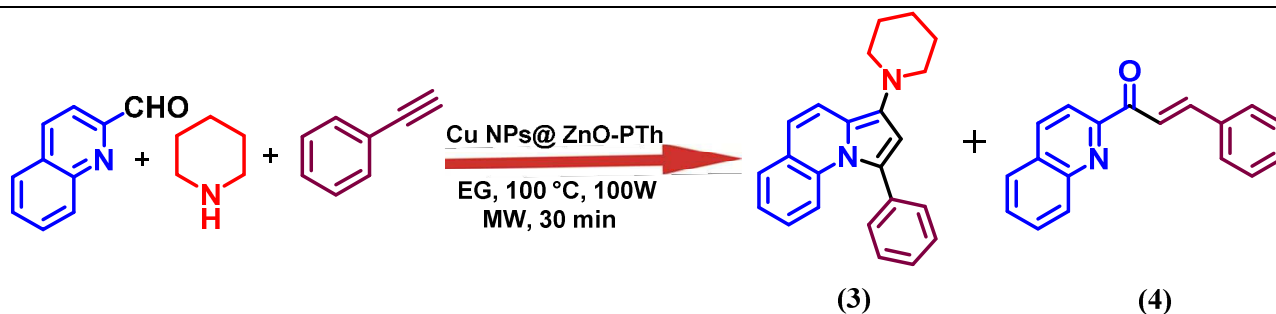
To achieved the excellent catalytic performance of the present catalyst towards the A³ and KA² coupling reaction, we further extended the versatility of CuNPs@ZnO-PTh catalyst for the

synthesis of pyrrolo[1, 2-a]quinoline as represented in Scheme 3. A model reaction of quinoline-2-carboxaldehyde, piperidine, phenyl acetylene was used to synthesize pyrrolo[1, 2-a]quinoline. To optimize the reaction condition, various solvents were screened at 100°C in a model reaction as shown in Table 5.



Scheme 3 Cu NPs@ZnO-PTh Catalyzed Synthesis of Pyrrolo[1, 2a]quinoline via A³ Coupling Reaction.

In the presence of acetone, methanol, ethanol, a mixture of pyrrolo[1, 2-a]quinoline (A) and chalcone (B) were obtained (entries 2-4, Table 5). However, the chalcone formed more exclusively in case of solvent free conditions and H₂O in 55% and 50% yield respectively (Entries 1, 6, Table 5). To our delight, the selectivity in formation of desired product (A) was observed in the presence of DMF, acetonitrile, 1,4-dioxane and EG (Entries 5, 7-9, Table 5). The presence of catalyst was necessary for the progress of the reaction, as in its absence no reaction occurred (Entry 15, Table 5). The model reaction was performed with Cu NPs. However, poor conversion was observed (Entry 19, Table 5). In addition, the following reaction was also performed with ZnO-PTh, the trace amount of chalcone was obtained along with moderate yield of pyrrolo[1, 2-a]quinoline formation under optimized condition (Entry 20, Table 5).

Table 5 Optimization reaction conditions of synthesis of pyrrolo[1, 2-a]quinoline catalyzed by CuNPs@ZnO-PTh^a

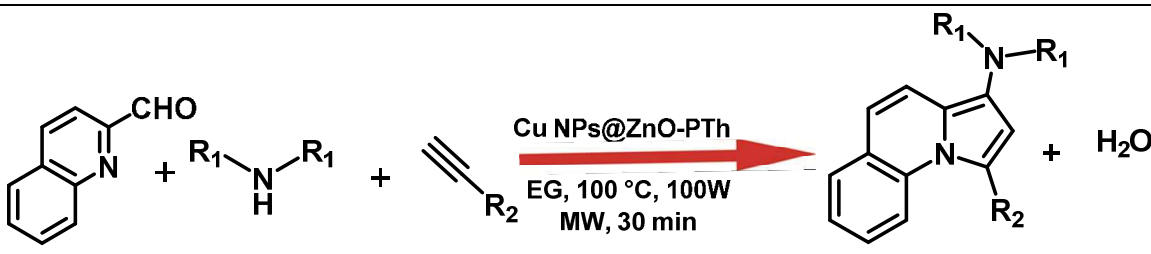
Entry	Catalyst(mg)	Solvent	Time (min)	Temp (°C)	Yield (%) (3)	Yield (%) (4)
1 ^b	20	-	30	100	-	55
2	20	Acetone	30	100	15	45
3	20	MeOH	30	100	54	19
4	20	EtOH	30	100	58	15
5	20	DMF	30	100	64	-
6	20	H ₂ O	30	100	-	50
7	20	Acetonitrile	30	100	75	-
8	20	1,4-dioxane	30	100	87	-
9	20	EG	30	100	98	-
10	20	EG	45	60	42	-
11	20	EG	40	70	65	-
12	20	EG	40	80	72	-
13	20	EG	30	90	87	-
14	20	EG	30	100	98	-
15 ^c	-	EG	30	100	Trace	-
16	05	EG	30	100	45	-
17	10	EG	30	100	64	-
18	15	EG	30	100	82	-
19 ^d	20	EG	30	100	24	-
20 ^e	20	EG	40	100	Trace	-

^aReaction conditions: Quinoline 2-carboxaldehyde (1.0 mmol), Piperidine (1.0 mmol), Phenyl acetylene (1.0 mmol), Catalyst (mol %), ^b = Solvent free conditions, ^c = Absence of catalyst.

^d = Presence of Cu NPs, ^e = Presence of ZnO-PTh.

The generality of CuNPs@ZnO-PTh catalytic system was studied for the synthesis of variety of pyrrolo[1,2-a]quinoline derivatives from the reaction among various substrates such as quinoline-2-carboxaldehyde, phenyl acetylenes and secondary amines under optimized reaction conditions as summarized in Table 6. The results indicates that the all screened substrates underwent smooth cycloisomerization to afford the pyrrolo[1, 2-a]quinoline with excellent yield (85-99%) (Table 6).

Table 6 Scope of the CuNPs@ZnO-PTh catalyst for the synthesis of pyrrolo[1, 2-a]quinoline



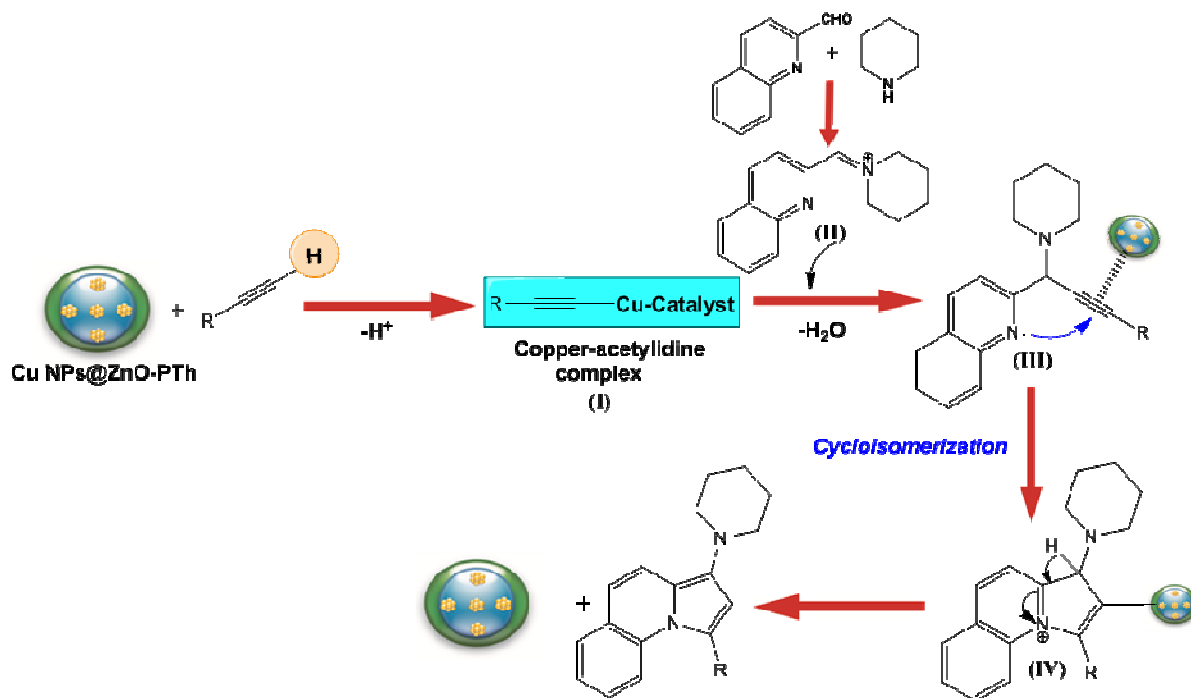
Entry	R ₁ (Amine)	R ₂ (Alkyne)	Yield (%)
1	Piperidine	Ph	98
2	Piperidine	4-Br-C ₆ H ₄	90
3	Piperidine	4-NO ₂ -C ₆ H ₄	85
4	Piperidine	C ₃ H ₅	90
15	Piperidine	4-OCH ₃ -C ₆ H ₄	99
6	Piperidine	4-CH ₃ -C ₆ H ₄	99
7	Pyrrolidine	Ph	95
8	Morpholine	Ph	92
9	4-Cyclohexyl Piperidine	Ph	94

Reaction conditions: Quinoline 2-carboxaldehyde (1.0 mmol), Acetylene (1.0 mmol), Secondary amine (1.0 mmol), Catalyst (20 mg), 5 mL EG, 30 min, 100 W.

Proposed reaction mechanism for CuNPs@ZnO-PTh catalyzed synthesis of pyrrolo [1,2a]quinolines

Based on the literature reports, we proposed the mechanism for three component one pot synthesis of propargylamine over CuNPs@ZnO-PTh nanocomposite. The probable reaction mechanistic scheme was pictorially illustrated in Scheme 4. In step I, it was proposed that Cu

nanoparticles on ZnO-PTh support activate the C–H bond of the acetylenic substrate to generate a copper-acetylide complex on the surface of ZnO-PTh support²³. This was indeed a very favourable step because copper is well known to exhibit high alkynophilicity for terminal alkynes. In step II, the copper-acetylide complex reacts with iminium ions that were generated *in-situ* from the reaction between aldehyde and secondary amine, to give corresponding 2-quinolinyl propargylamine intermediate. The cyclo-isomerization of intermediate (III) can be promoted by copper active sites of CuNPs@ZnO-PTh to afford the desired product. The catalytic activity of CuNPs@ZnO-PTh may be due to the synergistic effect of both Cu nanoparticle and ZnO-PTh active site. The CuNPs@ZnO-PTh catalyst gets regenerated which further enabled catalytic cycles to continue till the completion of the reaction. Moreover, the synergistic effect of both the ZnO-PTh and CuNPs was responsible for its excellent catalytic activity.



Scheme 4 Plausible reaction mechanism for the one pot synthesis of propargylamines using CuNPs@ZnO-PTh catalyst

Green chemistry metrics

The green chemistry metrics are the important parameter for the evaluation of green and sustainable reaction. The green chemistry metrics for all three model reactions to form propargylamine (1), tetra substituted propargylamine (2) and pyrrolo[1, 2-a]quinoline (3) were calculated and the results were represented in Table 4 (Calculation provided in ESI). The results

indicated that the values of green chemistry metrics such as E-factor, process mass intensity (PMI), reaction mass efficiency (RME), atom economy (AE), and carbon efficiency (CE) were almost close to their ideal values.⁶⁶⁻⁶⁷

Table 7 Quantification of Green chemistry metrics for the product (1), (2) and (3)

No	Green Chemistry Metrics	Ideal value	Product (1)	Product (2)	Product (3)
1	E-factor	0	0.0892	0.087	0.075
2	Process mass intensity (PMI)	1	1.089	1.087	1.075
3	Reaction mass efficiency (RME)	100 %	92 %	92 %	93 %
4	Atom economy (AE)	100 %	94%	94 %	95 %
5	Carbon efficiency (CE)	100 %	98 %	98 %	98 %

Recyclability

The catalyst separation and its reusability were the most important parameters for an ideal heterogeneous catalytic system that made the protocol more economical and sustainable over homogeneous catalysts. The recyclability of CuNPs@ZnO-PTh catalysts has been evaluated for the synthesis of propargylamine (A^3 coupling) under the optimised reaction conditions. (Figure 10).

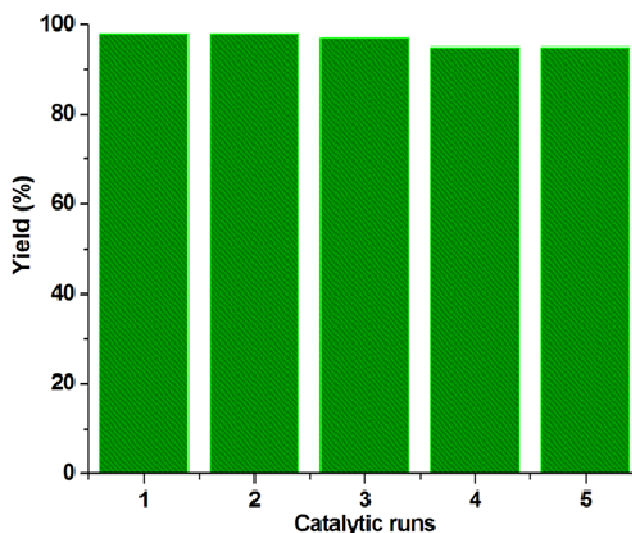


Figure 10 Recycling of CuNPs@ZnO-PTh catalyst in the A³ coupling

The catalyst was recovered after the completion of reaction by using centrifugation method and washed with hot distilled water and methanol to remove the absorbed products. After that, it was dried under vacuum and further reused to check its catalytic activity. The catalytic property of nanocomposite was studied for five consecutive cycles without any significant loss in product yield. It has been noted that in first four cycles, the loss of its activity was negligible. After the fifth cycle, there was a slight reduction of 3 % from the initial catalytic activity which indicates sustainability of nanocomposites. TEM analysis of the recycled catalyst was another important technique to ascertain the particle size of metal nanoparticles after the reaction. TEM images of the recovered catalyst after the fifth cycles shows that most of the particles were still in the size range of 2-7 nm. However, some bigger particles and slight agglomeration of copper nanoparticles was also found within the size range of 10-15 nm (Figure 11). This implies that, growth occurs by copper nanoparticles migration and coalescence that was mostly viable at the exposed surface of ZnO-PTh nanocomposite.

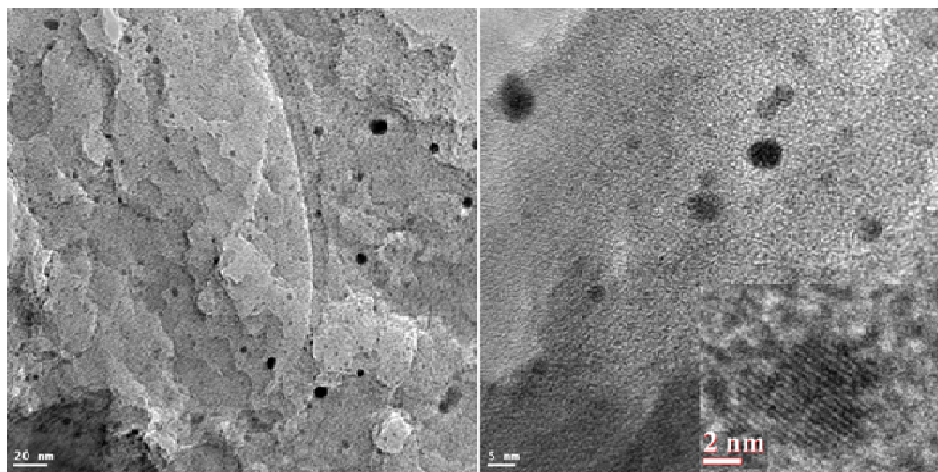


Figure 11 TEM and HR-TEM images of recycled CuNPs@ZnO-PTh catalyst

Comparison of catalytic activity of supported copper nanoparticles towards the synthesis of Propargylamine

The catalytic activities of CuNPs@ZnO-PTh for the synthesis of propargylamine with that of previous work related to copper based catalyst with different supports are compared (Table 8). It was observed that the yield of propargylamine achieved using this catalyst was comparable to those reported earlier in literature. The solvent used for this protocol was biodegradable and reusable. Furthermore, the minimum reaction time was required to afford higher yield of propargylamine. Present work reports only 0.0052 % of Cu (25 mg of Cu NPs/ZnO-PTh) which is substantially low as compared to other catalysts.

Table 8 Comparison of catalytic activity of copper nanoparticles deposited on different supports

Entry	Catalyst	Cu (Mol %)	Solvent	Temp (°C)	Time	Yield (%)	Ref.
1	Cu NPs/MS	0.3	THF	60	20 h	96	36
2	Cu NPs/TiO ₂	0.5	Neat	70	7 h	98	37
3	CuO/GNS	0.7	Acetonitrile	82	5 h	89	43
4	Cu/Nitro Resin	0.0037	Toluene	100	25 min	98	53
5	Cu NPs/MOF-5-C	9.7	Toluene	110	6 h	96	68
6	Cu/PMO-IL	0.15	CHCl ₃	60	24 h	97	69
7	Cu/Montmorillonite	0.05	Toluene	110	3 h	98	46
8	Cu/NCNTs	0.004	THF	70	4-6 h	85	70

9	Cu/Graphene	2.6	Toluene	100	24 h	96	71
10	Cu NPs/ZnO-PTh	0.0052	EG	80	15 min	98	Present Work

MS = Starch Microparticles, GNS = Graphene Nano sheet, NCTs = Nitrogen-doped carbon nanotubes

Study of catalytic leaching is another important parameter to determine the recyclability of heterogeneous catalyst. Leaching of active metal species mostly depends upon number of circumstances such as type of solvent and stabilizing agents that used during the reaction. To estimate the leaching of copper from the catalyst material, the filtrate was analyzed by ICP-AES after the removal of catalyst from the reaction mixture. No trace of copper was observed above the detectable limit. This indicates that there were no stable catalytic species in the reaction mixture. In addition, it was revealed that the concentration of copper present in fresh catalyst was similar as compared to reused catalyst at fifth cycle.

Conclusion

The present work develops an efficient protocol for the synthesis of CuNPs@ZnO-PTh via a simple impregnation method using inexpensive starting material, which is an important criteria for large scale industrial productions. The catalytic properties of CuNPs@ZnO-PTh was investigated for the synthesis of propargylamine, tetra substituted propargylamine (A^3 and KA^2 coupling reactions) and pyrrolo[1, 2-a]quinoline (A^3 coupling reactions). CuNPs@ZnO-PTh catalyst with loading (20-25 mg) shows highest yield of desired product in minimum reaction time (98%, 15 min) at 80°C in ethylene glycol as green solvent. The high surface area and synergistic effect of both the ZnO-PTh and CuNPs was responsible for its excellent catalytic performance along with wide substrate scope, mild reaction conditions, recyclability without significant loss in activity, short reaction time, easy work-up procedure, green solvent free conditions with higher yield. Further, applications in drug design of synthesized molecules are currently ongoing with collaboration.

Acknowledgement

One of the authors (A. Shah) is thankful to the University Grants Commission, New Delhi, India for providing financial support under the MANF (Maulana Azad National Fellowship). Also

thankful to NCNNU, University of Mumbai, PRL, Ahmedabad and MNIT Jaipur for providing characterization facilities.

References

1. K. Wang, L. Yang, W. Zhao, L. Cao, Z. Sun and F. Zhang, *Green Chem.*, 2017, **19**, 1949-1957.
2. (a) A. Fedorov, H. Liu, H. Lo and C. Copéret, *J. Am. Chem. Soc.*, 2016, **138**, 16502-16507; (b) W. Gao, Y. F. Zhao, H. R. Chen, H. Chen, Y. W. Li, S. He, Y. K. Zhang, M. Wei, D. G. Evans and X. Duan, *Green Chem.*, 2015, **17**, 1525-1534.
3. B. J. Borah, D. Dutta, P. P. Saikia, N. C. Barua and D. K. Dutta, *Green Chem.*, 2011, **13**, 3453-3460.
4. (a) B. Rungtaweeworanit, J. Baek, J. R. Araujo, B. S. Archanjo, K. M. Choi, O. M. Yaghi and G. A. Somorjai, *Nano Lett.*, 2016, **16**, 7645-7649; (b) K. S. Gayen, T. Sengupta, Y. Saima, A. Das, D. K. Maiti and A. Mitra, *Green Chem.*, 2012, **14**, 1589-1592.
5. (a) R. B. N. Baig and R. S. Varma, *Green Chem.*, 2012, **14**, 625-632; (b) R. Hudson, C. J. Li and A. Moores, *Green Chem.*, 2012, **14**, 622-624.
6. F. Wang, R. Shi, Z. Q. Liu, P. J. Shang, X. Pang, S. Shen, Z. Feng, C. Li and W. Shen, *ACS Catal.*, 2013, **3**, 890-894.
7. M. B. Gawande, A. Goswami, F.X. Felpin, T. Asefa, X. Huang, R. Silva, X. Zou, R. Zboril and R. S. Varma, *Chem. Rev.*, 2016, **116**, 3722-3811.
8. A. J. Canty, E. I. Negishi (Ed.), *Handbook of Organopalladium Chemistry*, vol. 1, Wiley, New York, 2002.
9. D. Deng, Y. Cheng, Y. Jin, T. Qi and F. Xiao, *J. Mater. Chem.*, 2012, **22**, 23989-23995.
10. G. A. Somorjai and J. Y. Park, *Angew. Chem. Int. Ed.*, 2008, **47**, 9212-9228.
11. A. Maleki, *Ultrason Sonochem.*, 2018, **40**, 460-464.
12. M. B. Gawande, S. N. Shelke, R. Zboril and R. S. Varma, *Acc. Chem. Res.*, 2014, **47**, 1338-1348.
13. N. E. Leadbeater, *J. Am. Chem. Soc.*, 2011, **133**, 2011-2011.
14. A. Maleki, *RSC Adv.*, 2014, **4**, 64169-64173.
15. A. Maleki, *Tetrahedron Lett.*, 2013, **54**, 2055-2059.
16. G. Brahmachari, K. Nurjamal, I. Karmakar, S. Begam, N. Nayek and B. Mandal, *ACS Sustainable Chem. Eng.*, 2017, **5**, 9494-9505.
17. R. A. Sheldon, *Green Chem.*, 2017, **19**, 18-43.
18. V. A. Peshkov, O. P. Pereshivkova and E. V. V. der Eycken, *Chem. Soc. Rev.*, 2012, **41**, 3790-3807.

19. Y. Imada, M. Ysusa, I. Nakamura and S. I. Murahashi, *J. Org. Chem.*, 1994, **59**, 2282-2284.
20. M. B. H. Youdim, O. Binah, Z. A. Abassi, Y. Barac, R. F. I. Technion Research and Development Foundation Ltd., EP1942881B1, 2012, 27.
21. A. A. Boulton, B. A. Davis, D. A. Durden, L. E. Dyck, A. V. Juorio, X. M. Li, I. A. Paterson and P. H. Yu, *Drug Dev. Res.*, 1997, **42**, 150-156.
22. C. Swithenbank, P. J. McNulty and K. L. Viste, *J. Agric. Food Chem.*, 1971, **19**, 417-421.
23. U. C. Rajesh, U. Gulati and D. S. Rawat, *ACS Sustainable Chem. Eng.*, 2016, **4**, 3409-3419.
24. C. Souccar, W. A. Varanda, R. S. Aronstam, J. W. Daly and E. X. Albuquerque, *Mol. Pharmacol.*, 1984, **25**, 384-94.
25. C. Wei and C. J. Li, *J. Am. Chem. Soc.*, 2002, **124**, 5638-5639.
26. H. B. Chen, Y. Zhao and Y. Liao, *RSC Adv.*, 2015, **5**, 37737-37741.
27. K. Zhang, Y. Huang and R. Chen, *Tetrahedron Lett.*, 2010, **51**, 5463-5465.
28. A. Bisai and V. K. Singh, *Org. Lett.*, 2006, **8**, 2405-2408.
29. A. Grirrane, E. Alvarez, H. Garcia and A. Corma, *Angew. Chem. Ed.*, 2014, **53**, 7253-7258.
30. N. Gommermann and P. Knochel, *Chem. Commun.*, 2005, **0**, 4175-4177.
31. S. B. Park and H. Alpher, *Chem. Comm.*, 2005, **0**, 1315-1317.
32. A. B. Dyatkin and R. A. Rivero, *Tetrahedron Lett.*, 1998, **39**, 3647-3650.
33. D. Yu and Y. Zhang, *Adv. Syn. Catal.*, 2011, **353**, 163-169.
34. X. Liu, B. Lin, Z. Zhang, H. Lei and Y. Li, *RSC Adv.*, 2016, **6**, 94399-94407.
35. M. Wang, P. Li and L. Wang, *Eur. J. Org. Chem.*, 2008, 2255-2261.
36. M. Gholinejad, F. Saadati, S. Shaybanizadeh and B. Pullithadathil, *RSC Adv.*, 2016, **6**, 4983-4991.
37. M. J. Albaladejo, F. Alonso, Y. Moglie and M. Yus, *Eur. J. Org. Chem.*, 2012, 3093-3104.
38. U. C. Rajesh, U. Gulati and D. S. Rawat, *ACS Sustainable Chem. Eng.*, 2016, **4**, 3409-3419.
39. U. Gulati, U. C. Rajesh and D. S. Rawat, *Tetrahedron Lett.*, 2016, **57**, 4468-4472.
40. U. C. Rajesh, V. S. Pawan and D. S. Rawat, *RSC Adv.*, 2016, **6**, 2935-2943.
41. H. Naeimi and M. Moradian, *Appl. Organomet. Chem.*, 2013, **27**, 300-306.
42. M. K. Patil, M. Keller, B. M. Reddy, P. Pale and J. Sommer, *Eur. J. Org. Chem.*, 2008, 4440-4445.

43. M. Gopiraman, D. Deng, S. G. Babu, T. Hayashi, R. KKarvembu and I. S. Kim, *ACS Sustainable Chem. Eng.*, 2015, **3**, 2478-2488.
44. S. Frindly, A. El Kedib, M. Lahcini, A. Primo and H. Garcia, *Catal. Sci. Tech.*, 2016, **6**, 4306-4317.
45. M. Mirabedini, E. Motamedi and M. Zaman Kassae, *Chin. Chem. Lett.*, 2015, **26**, 1085-1090.
46. B. J. Borah, S. J. Borah, L. Saikia and D. K. Dutta, *Catal. Sci. Tech.*, 2014, **4**, 1047-1054.
47. B. R. P. Reddy, P. V. G. Reddy, M. V. Shankar and B. N. Reddy, *Asian J. Org. Chem.*, 2017, **6**, 712-719.
48. M. H. Sarvari and F. Moeini, *New. J. Chem.*, 2014, **38**, 624-635.
49. J. Dulke, K. Thirunavukkarasu, M. C. M. Hazeleger, D. V. Andreeva, N. R. Shiju and G. Rothenberg, *Green. Chem.*, 2013, **15**, 1238-1243.
50. X. Xiong, H. Chen and R. Zhu, *Chinese J. Catal.*, 2014, **35**, 0-0. DOI: 10.1016/S1872-2067(14)60195-9
51. H. Feng, D. S. Ermolatev, G. Song and E. V. Van der Eycken, *J. Org. Chem.*, 2011, **76**, 7608-7613.
52. L. Shi, Y. Q. Tu, M. Wang, F. M. Zhang and C. A. Fan, *Org. Lett.*, 2004, **6**, 1001-1003.
53. A. S. Sharma, H. Kaur and N. Barot, *J. Phy. Org. Chem.*, 2017, e3749.
54. S. Jain, N. Karmakar, A. Shah, D.C. Kothari, S. Mishra and N. G. Shimpi, *Appl. Surf. Sci.*, 2017, **396**, 1317-1325.
55. M. Khatamian, M. Fazayeli and B. Divband, *Mater. Sci. Semicond. Process*, 2014, **26**, 540-547.
56. A. Maleki, A. A. Jafari, S. Yousefi, *J. Iran Chem. Soc.*, 2017, **14**, 1801-1813.
57. N.G. Shimpi, S. Jain, N. Karmakar, A. Shah, D. C. Kothari and S. Mishra, *Appl. Surf. Sci.*, 2016, **390**, 17-24.
58. K. Cheirmadurai, S. Biswas, R. Murali and P. Thanikaivelan, *RSC Adv.*, 2014, **4**, 19507-19511.
59. N. Barot, T. Shaikh and H. Kaur, *New J. Chem.*, 2017,**41**, 5347-5354.
60. N.S. Ramgir, D.J. Late, A.B. Bhise, M.A. More, I.S. Mulla, D.S. Jaog and K. Vijayamohanan, *J. Phys. Chem. B.*, 2006, **110**, 18236-18242.
61. C.L. Aravinda, S.M. Mayanna, P. Bera, V. Jarayam and A.K. Sharma, *J. Mater. Sci. Lett.*, 2002, **21**, 205-208.
62. K. Yoshida, C. Gonzalez-Arellano, R. Luque and P.L. Gai, *Appl. Catal. A.*, 2010, **379**, 38-44.
63. Z. Huang, F. Cui, H. Kang, J. Chen, X. Zhang and C. Xia, *Chem. Mater.*, 2008, **20**, 5090-5099.
64. A. Maleki, T. Kari, M. Aghaei, *J. Porous Mater.*, 2017, **24**, 1481-1496.

65. A. Maleki, H. Movahed, P. Ravahgi, *Carbohydr. Polym.*, 2017, 156, 259-267.
66. G. Purohit, U. C. Rajesh and D. Rawat, *ACS Sustainable Chem. Eng.*, 2017, **5**, 6466-6477.
67. P. T. Anastas and D. T. Allen, *ACS Sustainable Chem. Eng.*, 2016, **4**, 5820-5820.
68. S. Cheng, N. Shang, C. Feng, S. Gao, C. Wang and Z. Wang, *Cat. Comm.*, 2017, **89**, 91–95.
69. M. Gholinejad, B. Karimi, A. Aminianfar, and M. Khorasani, *Chem. Plus. Chem.*, 2015, **80**, 1573 – 1579.
70. V. G. Ramu, A. Bordoloi, T. C. Nagaiah, W. Schuhmann, M. Muhler, C. Cabrele, *Appl. Catal. A- Gen.*, 2012, **431-432**, 88–94.
71. S. Frindy, A. E. Kadib, M. Lahcini, A. Primo, H. García, *Catal. Sci. Technol.*, 2016, **6**, 4306-4317.

Graphical abstract

Cu@ZnO-PTh nanocomposite was synthesized and used as a heterogeneous catalyst for KA² and A³ coupling which is highly efficient and green technique.

